Nuclear spin blockade of laser ignition of intramolecular rotation in the model boron rotor $^{11}B_{13}^{+}$

Thomas Grohmann,[1,2] Dietrich Haase,[2] Dongming Jia,[1,a)] Jörn Manz,[1,2,3] and Yonggang Yang[1,3]

[1]*State Key Laboratory of Quantum Optics and Quantum Optics Devices, Institute of Laser Spectroscopy, Shanxi University, 92, Wucheng Road, Taiyuan 030006, China*
[2]*Institut für Chemie und Biochemie, Freie Universität Berlin, Takustrasse 3, 14195 Berlin, Germany*
[3]*Collaborative Innovation Center of Extreme Optics, Shanxi University, 92, Wucheng Road, Taiyuan 030006, China*

(Received 13 July 2018; accepted 12 October 2018; published online 13 November 2018)

The boron rotor $^{11}B_{13}^{+}$ consists of a tri-atomic inner "wheel" that may rotate in its pseudo-rotating ten-atomic outer "bearing"—this concerted motion is called "contorsion." $^{11}B_{13}^{+}$ in its ground state has zero contorsional angular momentum. Starting from this initial state, it is a challenge to ignite contorsion by a laser pulse. We discover, however, that this is impossible, i.e., one cannot design any laser pulse that induces a transition from the ground to excited states with non-zero contorsional angular momentum. The reason is that the ground state is characterized by a specific combination of irreducible representations (IRREPs) of its contorsional and nuclear spin wavefunctions. Laser pulses conserve these IRREPs because hypothetical changes of the IRREPs would require nuclear spin flips that cannot be realized during the interaction with the laser pulse. We show that all excited target states of $^{11}B_{13}^{+}$ with non-zero contorsional angular momentum have different IRREPs that are inaccessible by laser pulses. Conservation of nuclear spins thus prohibits laser-induced transitions from the non-rotating ground to rotating target states. We discover various additional constraints imposed by conservation of nuclear spins, e.g., laser pulses can change clockwise to counter-clockwise contorsions or vice versa, but they cannot stop them. The results are derived in the frame of a simple model. *Published by AIP Publishing.* https://doi.org/10.1063/1.5048358

I. INTRODUCTION

This paper has two motivations that are somewhat antagonistic: On the one hand, it is a rewarding task to ignite intramolecular rotations in molecular rotors. Impressive experimental demonstrations are documented in Refs. 1–4 supplemented by theoretical concepts.[5–8] A particular challenge here is the laser excitation of rotations in the planar boron rotors B_{11}^{-},[9,10] B_{13}^{+},[11–14] B_{15}^{+},[15] and B_{19}^{-}.[16–18] Pictorially speaking, these rotors consist of a small inner "wheel" that rotates fluxionally in an outer "bearing." If the rotary motion starts out from a global minimum (GM) structure, then it transforms the initial GM to another one and then to a third one, and so on. The mobility of these rotors is supported by two properties: First, by their rather low (typically below 1 kcal/mol[9–18]) potential barriers or transition states (TSs) between potential wells that support the GM structures. These potential wells and their GMs as well as the TSs between the GMs are arranged in cyclic orders, GM_1, $TS_{1,2}$, GM_2, $TS_{2,3}$, ..., GM_N, $TS_{N,1}$, where the total numbers N of the GMs and TSs are rather large: They are equal to the product $N = N_w \times N_b$ of the number N_w of atoms that determines the shape of the wheel times the number of atoms N_b in the bearing; thus, $N = 2 \times 9$, 3×10, 4×11, and 5×13 for B_{11}^{-}, B_{13}^{+}, B_{15}^{+}, and B_{19}^{-}, respectively. Second, the mobility is supported by pseudo-rotations of the nuclei of the bearings that adapt their shape to the rotating wheel,[19,20] which is analogous to rotating molecules in pseudo-rotating cages.[21] According to the terminology that has been introduced in Ref. 22 in accordance with the nomenclature that was coined in Ref. 23, the concerted rotational (or torsional) and pseudo-rotational motion of the boron rotors will be called "contorsion" below. The boron rotors were given names that point to their rotary mobility, such as molecular "Wankel motors,"[12,13,17,18] "tank treads"[9,15] with the peripheral atoms behaving as a flexible "chain gliding around," or "molecular ball bearings."[14] The rotary motions were demonstrated by means of molecular dynamics (MD) simulations;[9,10,12,14,15,17,18] these employ classical trajectories that are propagated on the potential energy surfaces of the molecular rotors in their electronic ground states. Recently, Fagiani *et al.* discovered two signatures of the mobility of B_{13}^{+} in infrared (IR) spectra, namely, apparent line broadening and a spectral peak that was assigned to the rotor when it crosses the TS.[14] Zhang *et al.* suggested to trigger the intramolecular rotation of B_{13}^{+} by means of an external laser field, with MD simulations of the mechanism.[12] Their concept was highlighted by Merino and Heine's article entitled "And yet it rotates: The starter for a molecular Wankel motor."[13]

On the other hand, recently, Grohmann and Manz have discovered fascinating effects of the nuclear spins of the boron

a)Electronic mail: dmjia@email.sxu.edu.cn

rotors that render the previous results of classical MD simulations assailable.[22] They investigate explicitly the example $^{11}B_{11}^-$ using the theory of molecular symmetry (MS) groups[23] and a simple model and extrapolate analogous results for all planar boron rotors.[11–20] Their model extends that of Refs. 19 and 20 by considering not only the contorsions of the rotors but also the constraints imposed by nuclear spins. Analogous constraints are described in many textbooks of quantum mechanics and physical chemistry, usually for the hydrogen molecule with its two nuclear spin isomers, *para*-H_2 and *ortho*-H_2. For reference, Fig. 1 shows the energy levels of the lowest rotational states of *para*-H_2 and *ortho*-H_2, together with a hypothetical transition for rotational excitation by a right circularly polarized laser pulse, for example, from the ground state $JM = 00$ (*para*-H_2) to the first excited rotational state $JM = 11$ (*ortho*-H_2). This type of rotational excitation is doubly prohibited: First, it is "dipole forbidden" because the electric dipole $\boldsymbol{d}(R)$ of H_2 in the electronic ground state $^1\Sigma_g^+$ is exactly equal to zero for all molecular orientations and for all internuclear distances R. As a consequence, the interaction $-\boldsymbol{\varepsilon}\cdot\boldsymbol{d}$ between the laser field $\boldsymbol{\varepsilon}$ and the dipole $\boldsymbol{d}$ is equal to zero and the transition dipole matrix element $\langle\Psi_{011}|-\boldsymbol{\varepsilon}\cdot\boldsymbol{d}|\Psi_{000}\rangle$ between the vibrational and rotational ground state $\Psi_{\nu JM=000}$ and the target state $\Psi_{\nu' J' M'=011}$ vanishes. Second, the transition is prohibited by nuclear spins because it would call for nuclear spin flip; this is associated with a change of the symmetry (or the corresponding irreducible representations, IRREPs) of the nuclear spin wavefunctions, here from the nuclear singlet state (total nuclear spin quantum numbers I_{tot}, $m_{I_{\text{tot}}} = 0, 0$: *para*-$H_2$) to the triplet state ($I_{\text{tot}}$, $m_{I_{\text{tot}}} = 1, 1$: *ortho*-$H_2$). Now, on one hand, the familiar (first) dipole selection rule is actually an approximation that is derived by means of perturbation theory in the weak field limit and in the frame of the Born-Oppenheimer approximation (BOA). This can be overcome, in principle, by intense ultrashort laser pulses, beyond the BOA.[24,25] On the other hand, it is impossible to overcome the (second) selection rule imposed by the nuclear spins, during typical durations of laser pulses. Thus, for reference, it is actually the nuclear spins that block rotational $JM = 00 \rightarrow 11$ laser excitation of H_2. By contrast, transitions within the same nuclear spin isomer, e.g., from $\Psi_{\nu JM=000}$ (*para*-H_2) to $\Psi_{\nu' J' M'=020}$ (also *para*-H_2), conserve nuclear spin; hence, such transitions can be induced by means of an ultrashort intense laser pulse even though they are dipole-forbidden in the weak-field limit (cf. Fig. 1).

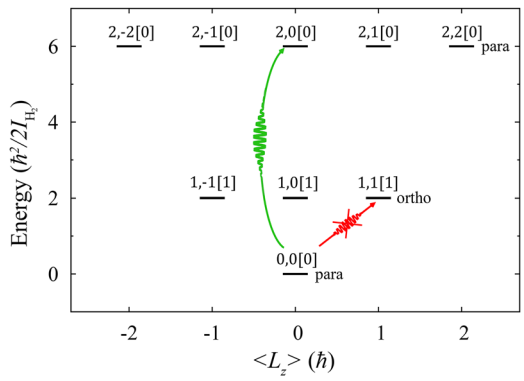

FIG. 1. The reference system: Nuclear spin blockade of hypothetical rotational laser excitation of H_2 from the ground state J, $M = 0, 0$ [$I_{\text{tot}} = 0$] (*para*-H_2) to the first excited state J, $M = 1, 1$ [$I_{\text{tot}} = 1$] (*ortho*-H_2). Transitions that conserve nuclear spin are not prohibited, e.g., from J, $M = 0, 0$ [$I_{\text{tot}} = 0$] (*para*-H_2) to J, $M = 2, 0$ [$I_{\text{tot}} = 0$] (*para*-H_2).

Analogous effects of nuclear spins were ignored in previous work on boron rotors;[9–20] see also the reviews Refs. 26 and 27. Here, we investigate these phenomena using the model of Refs. 19, 20, and 22 for planar boron rotors that consist of a single boron isotope, specifically ^{11}B with corresponding nuclear spin $\frac{3}{2}\hbar$, and that are aligned in a plane, say, in the x-y-plane of the laboratory; equivalent results hold for the less abundant isotope ^{10}B with nuclear spin $3\hbar$. These boron rotors have many more nuclear spin isomers than the familiar two species of H_2. Hence we do not call them "para" or "ortho," but they will be labeled by their irreducible representations $\Gamma_0, \Gamma_1, \ldots, \Gamma_{N-1}$; see Sec. II B. It turns out that the numbers N of nuclear spin isomers are equal to the numbers of GMs and TSs, that is, $N = 18$, 30, 44, and 65 for $^{11}B_{11}^-$, $^{11}B_{13}^+$, $^{11}B_{15}^+$, and $^{11}B_{19}^-$, respectively.[22] Explicitly, we shall consider the example of the aligned boron rotor $^{11}B_{13}^+$, i.e., the system that was also investigated in Refs. 11–14 and 20.

Important details of the scenario and the model will be specified in Sec. II. Suffice it here to say that we consider the rotor at contorsional energies well below any electronic or in-plane vibrational excitations and the model neglects interactions of nuclear spins that take much longer times than typical durations of laser pulses, as well as couplings of contorsions and complementary vibrations, as explained in Ref. 22. Using this model, Grohmann and Manz have shown that nuclear spins prohibit localized preparations of the boron rotors in a single GM structure.[22] The reason is that a hypothetical GM structure would have to be a superposition of eigenstates of all nuclear spin isomers $\Gamma_0, \ldots, \Gamma_{N-1}$—but this is not allowed, which is analogous to the nuclear spin blockade against any hypothetical superposition of eigenstates of *para*-H_2 and *ortho*-H_2. Instead, the boron rotors are always delocalized in all possible GM structures; for example, $^{11}B_{13}^+$ is always delocalized in all thirty GM structures.[22] Now, the classical trajectories of the previous MD simulations of boron rotors necessarily start out from a single GM structure. Yet, this type of initial preparation is prohibited by the nuclear spins, which were ignored in MD simulations.[22] In particular, the previous MD simulation of the ignition of intramolecular rotation in $^{11}B_{13}^+$ by means of electric fields,[12] which means the "starter for a molecular Wankel motor,"[13] appears assailable.

The conflict of the two antagonistic motivations for this paper is now clear. This raises the question whether one can really induce intramolecular rotations, such as in the aligned model rotor $^{11}B_{13}^+$, by means of well-designed laser pulses, starting from the non-rotating ground state of the rotor. We shall investigate this problem by using the model and the derivations of Ref. 22. Important steps include the assignment of the molecular symmetry (MS) group and the irreducible representations (IRREPs) that label the nuclear spin isomers of $^{11}B_{13}^+$, as well as the use of several equivalent representations of the operators of the MS group. The purpose

here is not to provide the ultimate answer—this could not be expected from the simple model. Instead, the answer derived within the frame of the model should stimulate extended investigations. On the way, we shall reveal additional constraints on contorsional transitions in $^{11}B_{13}^+$ imposed by nuclear spins. The model and methods are presented in Sec. II, the results and discussions in Sec. III, and the conclusions in Sec. IV.

II. MODEL AND METHODS

A. Contorsional eigenfunctions, energies, quantum numbers, and delocalized structures of the model rotor $^{11}B_{13}^+$

The planar boron rotor $^{11}B_{13}^+$ in its contorsional ground state is illustrated in Fig. 2(a) (adapted from Ref. 19), aligned in the *x*-*y* plane. For reference, one of the GM's is illustrated in Fig. 2(b). Here one recognizes the inner "wheel" with $N_w = 3$ boron atoms, embedded in the outer "bearing" with $N_b = 10$ boron atoms. So $^{11}B_{13}^+$ has altogether $N_b \times N_w = 30$ GM structures. The contorsion of $^{11}B_{13}^+$, which means the concerted rotation of the wheel with respect to the bearing combined with the pseudo-rotation of the nuclei of the bearing, is described as motion along the cyclic contorsional angle ξ, $0 \leqslant \xi \leqslant 2\pi$.[19,20] The value of the corresponding effective moment of inertia, $I_{\text{eff}} = 88.5\ \mu\text{Å}^2$, is adapted from Ref. 20. If the GM shown in Fig. 2(b) is labeled GM_1 and centered at $\xi_1 = \frac{2\pi}{2N} = \frac{2\pi}{60}$ ($\hat{=}\ 6°$), then the cyclic series GM_1, GM_2, ..., GM_k, ..., GM_N are centered at $\xi_k = \xi_1 + (k-1)\,\Delta\xi$, $k = 1, 2, \ldots, N = 30$, where $\Delta\xi = \frac{2\pi}{N} = \frac{2\pi}{30}$ ($\hat{=}\ 12°$). The corresponding transition states $TS_{1,2}$, $TS_{2,3}$, ..., $TS_{k,k+1}$, ..., $TS_{N,1}$ between the GMs are located at $\xi_{k,k+1} = k\,\Delta\xi$, $k = 1, 2, \ldots, N$ ($\hat{=}\ 12°, 24°, \ldots, 360° \equiv 0°$). The superposition of the localized structures of all GM_k yields the delocalized structure of the contorsional ground state that is illustrated in Fig. 2(a).

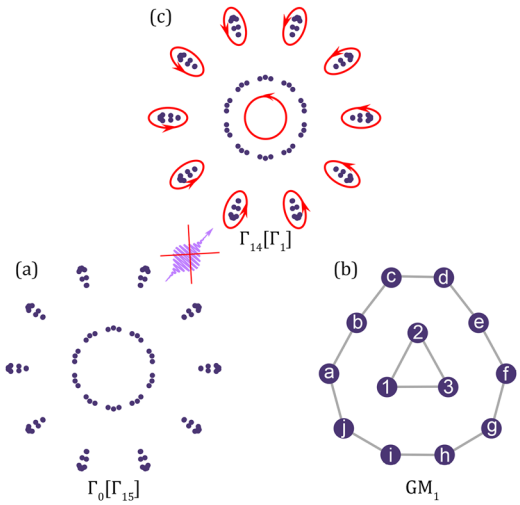

FIG. 2. (a) The planar boron rotor $^{11}B_{13}^+$ in its non-rotating ground state. This is realized for the nuclear spin isomer with irreducible representations (IRREPs) $\Gamma_0[\Gamma_{15}]$ of the contorsion [and nuclear spins]; see Sec. II C. Its delocalized structure comprises the superposition of thirty global minimum (GM) structures. As an illustration, one of them (GM_1) is shown in panel (b). (b) The GM structure GM_1 of $^{11}B_{13}^+$. The nuclei of its inner wheel and of the outer bearing are labeled 1, 2, 3 and a, b, c, ..., j, respectively. (c) The planar boron rotor $^{11}B_{13}^+$ in one of its excited states—here for the nuclear spin isomer with IRREPs $\Gamma_{14}[\Gamma_1]$. The arrows indicate the contorsional motions, i.e., the rotation of the inner wheel with respect to the bearing, and the concerted pseudo-rotations of the nuclei of the outer bearing. Hypothetical laser excitations from the non-rotating nuclear spin isomer $\Gamma_0[\Gamma_{15}]$ to the rotating nuclear spin isomer $\Gamma_{14}[\Gamma_1]$ or others are blocked by the nuclear spins, analogous to nuclear spin blockade of transitions between *para*- and *ortho*-H_2 illustrated in Fig. 1.

The contorsional eigenfunctions $\Phi_m(\xi)$ and energies E_m of the model boron rotor $^{11}B_{13}^+$ with quantum numbers $m = 0, 1, 2, \ldots$ are obtained as solutions of the Schrödinger equation

$$H_c\Phi_m(\xi) = E_m\Phi_m(\xi) \tag{1}$$

subject to cyclic boundary conditions $\Phi_m(\xi = 0) = \Phi_m(\xi = 2\pi)$. The contorsional model Hamiltonian is[19,20]

$$H_c = -\frac{\hbar^2}{2I_{\text{eff}}}\frac{d^2}{d\xi^2} + V(\xi). \tag{2}$$

The cyclic contorsional thirty-well potential $V(\xi)$ supports the thirty equivalent GM structures of $^{11}B_{13}^+$, separated by thirty equivalent TSs. It is modeled as[19,20]

$$V(\xi) = \frac{V_b}{2}[1 + \cos(30\xi)] \tag{3}$$

with barrier height $V_b = 106.4\,hc\ \text{cm}^{-1}$ adapted from Ref. 20; h is Planck's constant, and $c = c_0$ is the velocity of light in *vacuo*. The model potential (3) may be considered as the leading term of a symmetry-adapted Taylor expansion of the accurate potential; higher order terms $V_k\cos(30k\xi)$, $k = 2, 3, \ldots$, would induce irrelevant marginal shifts of the energies E_m, but they would not affect any of the fundamental results, e.g., they would not change the block-diagonal structure of the Hamiltonian matrix [see Eq. (9)] and the corresponding assignments of quantum numbers.

The wavefunctions will occasionally be written using Dirac notation, $\Phi_m(\xi) = \langle\xi|\Phi_m\rangle$. They are normalized and orthogonal,

$$\langle\Phi_m|\Phi_{m'}\rangle = \int_0^{2\pi} d\xi\,\Phi_m^*(\xi)\Phi_{m'}(\xi) = \delta_{m,m'}, \tag{4}$$

where $\delta_{m,m'}$ denotes Kronecker's symbol. They may be expanded in terms of ortho-normal contorsional basis functions

$$\phi_k(\xi) = \frac{1}{\sqrt{2\pi}}e^{ik\xi} \tag{5}$$

and thus

$$\Phi_m(\xi) = \sum_k c_{k,m}\phi_k(\xi). \tag{6}$$

Inserting the variational ansatz (6) into the Schrödinger equation (1) yields its algebraic version

$$\boldsymbol{H}\boldsymbol{c}_m = \boldsymbol{c}_m E_m, \tag{7}$$

with the vector $\boldsymbol{c}_m$ of the coefficients $c_{k,m}$ and with Hamilton matrix $\boldsymbol{H}$. Its elements are

$$H_{k,k'} = -\frac{\hbar^2}{2I_{\text{eff}}}k^2\delta_{k,k'} + \frac{1}{2}V_b\delta_{k,k'} + \frac{1}{4}V_b(\delta_{k,k'+30} + \delta_{k,k'-30}). \tag{8}$$

The Kronecker δ's in Eq. (8) make $\boldsymbol{H}$ rather sparse so that it can be written as a block diagonal matrix or as the corresponding direct sum of the block matrices

$$\boldsymbol{H} = \boldsymbol{H}_0 \oplus \boldsymbol{H}_1 \oplus \cdots \oplus \boldsymbol{H}_{29}, \tag{9}$$

where $\boldsymbol{H}_n$ contains the matrix elements for $k, k' = \ldots, n-60, n-30, n, n+30, n+60, \ldots$ such that $k \bmod 30 = n$, $n = 0,1, 2, \ldots, 29$. The Schrödinger equation (7) can then be solved for each Hamilton block matrix separately, and the resulting energies and wavefunctions can be labeled by two quantum numbers, $m = nl$ where $n = 0, 1, \ldots, 29$ denotes the number for the block and $l = 0, 1, 2, \ldots$ denotes the lth energy level for the nth block,

$$\boldsymbol{H}_n \boldsymbol{c}_{nl} = \boldsymbol{c}_{nl} E_{nl}. \tag{10}$$

These quantum numbers nl will be given important physical meanings below. The expansion (6) is thus reduced to

$$\Phi_{nl}(\xi) = \sum_k c_{k,nl}\, \phi_k(\xi), \quad k \bmod 30 = n. \tag{11}$$

The matrix elements (8) imply that the block matrix $\boldsymbol{H}_n$ is the same as $\boldsymbol{H}_{30-n}$, $n = 1, 2, \ldots, 14$, except for the reverse order of the diagonal elements. As a consequence, $\boldsymbol{H}_n$ and $\boldsymbol{H}_{30-n}$, $n = 1, 2, \ldots, 14$, have the same eigenvalues, i.e., E_{nl} and $E_{(30-n)l}$ are pair-wise degenerate,

$$E_{nl} = E_{(30-n)l} \text{ for } n = 1, 2, \ldots, 14, \tag{12}$$

whereas E_{0l} and E_{15l} are non-degenerate. Moreover, the coefficients for the degenerate eigenstates labeled nl and $(30-n)l$ appear in reverse order,

$$c_{k,nl} = c_{-k,(30-n)l}, \tag{13}$$

for $k \bmod 30 = n$ or $-k \bmod 30 = 30 - n$ with $n = 1, 2, \ldots, 14$. For the non-degenerate states, the symmetry relation $H_{kk} = H_{-k,-k}$ of the block diagonal matrices $\boldsymbol{H}_0$ and $\boldsymbol{H}_{15}$ imposes the related symmetries of the coefficients,

$$\begin{aligned} c_{k,0l} &= c_{-k,0l} \quad \text{or} \\ c_{k,0l} &= -c_{-k,0l} \quad \text{and} \quad c_{0,0l} = 0 \end{aligned} \tag{14}$$

for $k \bmod 30 = 0$, and

$$\begin{aligned} c_{k,15l} &= c_{-k,15l} \quad \text{or} \\ c_{k,15l} &= -c_{-k,15l} \end{aligned} \tag{15}$$

for $k \bmod 30 = 15$. These symmetry relations imply that the non-degenerate eigenfunctions $\Phi_{0l}(\xi)$ and $\Phi_{15l}(\xi)$ of the model boron rotor $^{11}B^+_{13}$ are real-valued, or they can be chosen to be real-valued, except for an irrelevant overall phase factor.

At first glance, the degeneracy of the two eigenstates, Eq. (12), may suggest that one could generate alternative pairs of degenerate contorsional eigenstates by means of a unitary transformation of the set of eigenfunctions $\Phi_{nl}(\xi)$ and $\Phi_{(30-n)l}(\xi)$. In the supplementary material with Refs. 28–36, we show, however, that one can prepare the "original" eigenfunctions that are obtained as solutions of the block diagonal Hamiltonians $\boldsymbol{H}_n$ and $\boldsymbol{H}_{30-n}$ in a unique manner by means of a magnetic field $\boldsymbol{B} = B_z \boldsymbol{e}_z$ that is oriented perpendicular to the molecular plane. Suffice it here to say that the field B_z lifts the degeneracy (12). The corresponding eigenfunctions $\Phi_{nl}(\xi; B_z)$ and $\Phi_{(30-n)l}(\xi; B_z)$ are determined, therefore, in a unique manner (that means without any option for unitary transformation). Finally, if one switches off the magnetic field adiabatically, the eigenfunctions $\Phi_{nl}(\xi; B_z \to 0)$ and $\Phi_{(30-n)l}(\xi; B_z \to 0)$ approach the original $\Phi_{nl}(\xi)$ and $\Phi_{(30-n)l}(\xi)$, with a continuous approach of the properties of $^{11}B^+_{13}$ in the magnetic field to $^{11}B^+_{13}$ without the magnetic field. In the context of the present investigation, the supplementary material shows, in particular, that the mean values of the canonical contorsional angular moment of $^{11}B^+_{13}$ in the magnetic field approach those that are calculated for $^{11}B^+_{13}$ without the magnetic field using the original solutions for the block diagonal Hamiltonians $\boldsymbol{H}_n$ and $\boldsymbol{H}_{30-n}$, $n = 1, 2, \ldots, 14$.

We close this subsection by a brief consideration of the numerical method for solving the Schrödinger equation (10) for the block diagonal Hamilton matrices $\boldsymbol{H}_n$. In principle, the expansion (11) is infinite and all the resulting Hamilton block matrices are infinite square matrices, but, in practice, they are truncated to finite basis sets, $k = n - N_n \times 30, \ldots, n-30, n, n+30, \ldots, n + (N_n - 1 + \delta_{n0}) \times 30$. Numerically converged results with accuracy better than 1/100 of the smallest level splitting are obtained for $N_n = 12$, which means the numerical square block matrix $\boldsymbol{H}_0$ is $2 \times 12 + 1 = 25$ dimensional, whereas all other block matrices are $2 \times 12 = 24$ dimensional.

B. The cyclic molecular symmetry group C_{30}(M) and the assignment of its irreducible representations to the contorsional eigenfunctions of $^{11}B^+_{13}$

Let us now consider the molecular symmetry (MS) group $G_{^{11}B^+_{13}}$(M) of the aligned model boron rotor $^{11}B^+_{13}$. It consists of all the feasible permutations of the three nuclei of the inner wheel (labeled 1, 2, and 3) and the ten nuclei of the outer bearing (labeled a, b, c, d, e, f, g, h, i, and j); see Fig. 2(b). According to Ref. 22, $G_{^{11}B^+_{13}}$(M) is the corresponding direct product of the cyclic groups of the inner wheel $C_{in} = C_3$(M) and the outer bearing $C_{out} = C_{10}$(M),

$$G_{^{11}B^+_{13}}(\mathrm{M}) = C_{in} \otimes C_{out} = C_{30}(\mathrm{M}). \tag{16}$$

We stress that even though contorting $^{11}B^+_{13}$ is planar, the inversion E^* is unfeasible in our scenario of pre-aligned boron rotors.[22]

The group C_{in} in Eq. (16) consists of the three feasible permutations

$$C_{in} = \{(1), (123), (132)\} = \{P^0_{in} = P^3_{in}, P_{in}, P^2_{in}\} \tag{17}$$

that are generated by the permutation

$$P_{in} = (123) \tag{18}$$

of the three nuclei of the inner wheel. Here we employ the so-called passive definition of permutations, e.g., (123) means that nucleus "1" is replaced by "2," "2" is replaced by "3," and "3" by "1." Likewise, C_{out} consists of ten feasible permutations of the nuclei a, b, c, ..., j of the outer bearing,

$$C_{out} = \{(a) = P^{10}_{out}, P^1_{out}, \cdots, P^9_{out}\}, \tag{19}$$

which are generated by

$$\mathrm{P_{out}} = (\mathrm{adgjcfibeh}). \tag{20}$$

See the Appendix.

The generator g of the direct product group (16) is the product of the generators of the sub-groups,

$$g = \mathrm{P_{in}}\,\mathrm{P_{out}} = (123)(\mathrm{adgjcfibeh}). \tag{21}$$

The cyclic MS group of $^{11}\mathrm{B}^{+}_{13}$ then consists of all 30 feasible permutations of its nuclei labeled 1, 2, 3, a, b, c, . . ., j that are generated by repeated applications of g,

$$\mathrm{G}_{^{11}\mathrm{B}^{+}_{13}}(\mathrm{M}) = \mathrm{C}_{30}(\mathrm{M}) = \{E = g^{30},\ g,\ g^2,\ \cdots,\ g^m,\ \cdots, g^{29}\}. \tag{22}$$

We have chosen the generator Eq. (21) such that the group elements E, g, g^2, . . ., g^m, . . ., g^{29} transform GM_1 into the cyclic sequence $\mathrm{GM}_1, \mathrm{GM}_2, \mathrm{GM}_3, \ldots, \mathrm{GM}_m, \ldots, \mathrm{GM}_{29}$. Thus we have

$$g\mathrm{GM}_1 = \mathrm{GM}_2, \tag{23}$$

$$g^m\mathrm{GM}_1 = \mathrm{GM}_{\mathrm{m+1}}, \tag{24}$$

$$g\mathrm{GM}_{\mathrm{m}} = \mathrm{GM}_{\mathrm{m+1}}. \tag{25}$$

Cyclic groups such as $\mathrm{C}_{30}(\mathrm{M})$ have various well-known properties that will be exploited below—for a summary that is tailored to the planar boron rotors, see Ref. 22. Specifically, $\mathrm{C}_{30}(\mathrm{M})$ has 30 one-dimensional IRREPs labeled Γ_0, Γ_1, . . ., Γ_n, . . ., Γ_{29}. The characters assigned to the group elements g^m are

$$\chi^{\Gamma_n}(g^m) = (\eta_{30}^m)^n, \tag{26}$$

where

$$\eta_{30} = e^{-2\pi\, i/30}. \tag{27}$$

This allows us to specify the IRREPs of $\mathrm{C}_{30}(\mathrm{M})$ by the characters of the generator,

$$\Gamma_n \leftrightarrow \chi^{\Gamma_n}(g) = \eta_{30}^n. \tag{28}$$

The relations (23)–(25) suggest equivalent alternative representations of the generator g and of the other group elements g^m of $\mathrm{C}_{30}(\mathrm{M})$, namely, in terms of the effect on the contorsional coordinate ξ, on the wavefunctions $\Phi_{nl}(\xi)$, $n = 0, 1, 2, \ldots, 29$, and on the underlying set of basis functions $\phi_k(\xi)$, k mod 30 = n, n = 0, 1, 2, . . ., 29. Since GM_1 and GM_2 in Eq. (23) [and likewise GM_m and GM_{m+1} in Eq. (25)] are centered at ξ_1 and $\xi_2 = \xi_1 + \Delta\xi$ (and likewise at ξ_m and $\xi_{m+1} = \xi_m + \Delta\xi$), respectively, we have

$$g\xi = \xi + \Delta\xi, \tag{29}$$

$$g^{-1}\xi = \xi - \Delta\xi, \tag{30}$$

$$g^m\xi = \xi + m\,\Delta\xi. \tag{31}$$

As a consequence,[37]

$$\begin{aligned} g\phi_k(\xi) &= \phi_k(g^{-1}\,\xi) = \phi_k(\xi - \Delta\xi) \\ &= \frac{1}{\sqrt{2\pi}} e^{i\,k(\xi-\Delta\xi)} = \eta_{30}^k \phi_k(\xi) \\ &= \eta_{30}^n \phi_k(\xi) \text{ if } k \bmod 30 = n. \end{aligned} \tag{32}$$

From Eq. (32), it follows that

$$\mathrm{IRREP}[\phi_k(\xi)] = \Gamma_n \text{ if } k \bmod 30 = n. \tag{33}$$

The expression (11) of the eigenfunctions $\Phi_{nl}(\xi)$ in terms of the basis functions $\phi_k(\xi)$ then implies that

$$\mathrm{IRREP}[\Phi_{nl}(\xi)] = \Gamma_n \tag{34}$$

or equivalently

$$\Gamma_n \leftrightarrow g\Phi_{nl}(\xi) = \eta_{30}^n\ \Phi_{nl}(\xi). \tag{35}$$

This allows us to assign physical meanings to the labels nl of the eigenfunctions $\Phi_{nl}(\xi)$ of the model $^{11}\mathrm{B}^{+}_{13}$ that are obtained as solutions of the Schrödinger equation (10) for the nth diagonal block of the Hamilton matrix $\boldsymbol{H}_n$, with energies E_{nl} and coefficients $\boldsymbol{c}_{nl}$: The quantum number $n = 0, 1, 2, \ldots, 29$ specifies the IRREP Γ_n, whereas $l = 0, 1, 2, \ldots$ specifies the level for the given Γ_n. We shall show below that the energies appear in groups, or "bands" of levels, i.e., all energies E_{n0}, $n = 0$, 1, . . ., 29, are well below the energies E_{n1}, $n = 0, 1, \ldots, 29$, and the latter are all below E_{n2}, $n = 0, 1, \ldots, 29$, etc. As a summary, the quantum numbers nl specify the IRREP Γ_n and the "energy band" l. The lowest and highest energies in each "band" are non-degenerate and all others are pair-wise degenerate [cf. Eq. (12)].

C. Molecular eigenfunctions of the model rotor $^{11}\mathrm{B}^{+}_{13}$

According to the nuclear spin hypothesis, molecular (mol) eigenfunctions can be written as products (or possibly as linear combinations of products) of rotational-contorsional-vibrational-electronic (rcve) times nuclear spin (nu.sp) eigenfunctions,[22,38]

$$\Phi^{\mathrm{mol}} = \Phi^{\mathrm{rcve}}\,\Phi^{\mathrm{nu.\,sp}}. \tag{36}$$

For the present simple model, the rcve-eigenfunctions are simply the contorsional eigenfunctions

$$\Phi^{\mathrm{rcve}}(\xi) = \Phi_{nl}(\xi) \tag{37}$$

assigned to the IRREP Γ_n and the energy band l.

The nuclear spin functions $\Phi^{\mathrm{nu.sp}} = \Phi^{\mathrm{nu.sp}}_{n'l'}$ have corresponding quantum numbers n' and l', which assign the IRREP $\Gamma_{n'}$ and specify the l'th wavefunction with IRREP $\Gamma_{n'}$. For details, see the supplementary material.

Having determined the contorsional eigenfunctions $\Phi^{\mathrm{rcve}}(\xi) = \Phi_{nl}(\xi)$ and the nuclear spin eigenfunctions $\Phi^{\mathrm{nu.sp}}(\Sigma_1,\ \Sigma_2,\ \Sigma_3,\ \Sigma_a,\ \Sigma_b,\ \ldots,\ \Sigma_j) = \Phi^{\mathrm{nu.sp}}_{n'l'}(\Sigma_1, \Sigma_2, \Sigma_3, \Sigma_a, \Sigma_b, \ldots, \Sigma_j)$, let us now consider the molecular eigenfunctions (36). For this purpose, it is mandatory to invoke the spin statistics theorem applied to the thirteen nuclei of the model boron rotor $^{11}\mathrm{B}^{+}_{13}$. These nuclei $^{11}\mathrm{B}$ are fermions because of the half-integer nuclear spin $I = \frac{3}{2}$. A familiar version of the spin statistics theorem for fermions is the requirement that the molecular wavefunction must change sign if one interchanges any two of the fermions.[39] Now let us consider the consequences of the theorem for the application of the generator g of the MS group $\mathrm{C}_{30}(\mathrm{M})$ applied to the molecular eigenfunctions of $^{11}\mathrm{B}^{+}_{13}$. The generator can be expressed in terms of eleven interchanges of two nuclei,

$$\begin{aligned} g &= (123)(\mathrm{adgjcfibeh}) \\ &= (13)(12)(\mathrm{ah})(\mathrm{ae})(\mathrm{ab})(\mathrm{ai})(\mathrm{af})(\mathrm{ac})(\mathrm{aj})(\mathrm{ag})(\mathrm{ad}). \end{aligned} \tag{38}$$

Hence,

$$\begin{aligned} g\Phi^{\text{mol}} &= (-1)^{11}\,\Phi^{\text{mol}} = -\Phi^{\text{mol}} \\ &= -\Phi_{nl}(\xi)\,\Phi^{\text{nu.sp}}_{n'l'}(\Sigma_1,\Sigma_2,\Sigma_3,\Sigma_a,\Sigma_b,\ldots,\Sigma_j) \\ &= \eta^{15}_{30}\,\Phi_{nl}(\xi)\,\Phi^{\text{nu.sp}}_{n'l'}(\Sigma_1,\Sigma_2,\Sigma_3,\Sigma_a,\Sigma_b,\ldots,\Sigma_j) \\ &= (g\,\Phi_{nl}(\xi))\,(g\Phi^{\text{nu.sp}}_{n'l'}(\Sigma_1,\Sigma_2,\Sigma_3,\Sigma_a,\Sigma_b,\ldots,\Sigma_j)) \\ &= \eta^{n}_{30}\,\Phi_{nl}(\xi)\,\eta^{n'}_{30}\,\Phi^{\text{nu.sp}}_{n'l'}(\Sigma_1,\Sigma_2,\Sigma_3,\Sigma_a,\Sigma_b,\ldots,\Sigma_j). \end{aligned} \tag{39}$$

A necessary condition for the validity of this application of the spin statistics theorem is

$$(n+n')\bmod 30 = 15. \tag{40}$$

As a consequence, one cannot combine the contorsional eigenfunction $\Phi_{nl}(\xi)$ with any arbitrary nuclear spin eigenfunction $\Phi^{\text{nu.sp}}_{n'l'}(\Sigma_1,\Sigma_2,\Sigma_3,\Sigma_a,\Sigma_b,\ldots,\Sigma_j)$. Instead, the IRREP Γ_n of $\Phi_{nl}(\xi)$ determines the IRREP $\Gamma_{n'}$ of $\Phi^{\text{nu.sp}}_{n'l'}(\Sigma_1,\Sigma_2,\Sigma_3,\Sigma_a,\Sigma_b,\ldots,\Sigma_j)$, and vice versa, such that n and n' satisfy condition (40). For example, if the IRREP of the contorsional eigenfunction is Γ_0, then the IRREP of the nuclear spin eigenfunction must be Γ_{15}. We denote this unique combination of the contorsional and nuclear spin IRREPs by $\Gamma_0[\Gamma_{15}]$. The corresponding nuclear spin isomer is thus labeled by $\Gamma_0[\Gamma_{15}]$. The definition of nuclear spin isomers in terms of their IRREPs is in accord with the convention that has been introduced in Refs. 40–43. The complete set of 30 nuclear spin isomers of $^{11}B^+_{13}$ are labeled by the IRREPs $\Gamma_n[\Gamma_{n'}]$ that satisfy condition (40); see also the supplementary material and, in particular, Table 1 for their numbers, $N^{\text{nu.sp}}[\Gamma_{n'}]$. Accordingly, the 30 nuclear spin isomers of the model rotor $^{11}B^+_{13}$ are labeled $\Gamma_n[\Gamma_{15-n}]$ for $n = 0, 1, 2, \ldots, 15$ and $\Gamma_n[\Gamma_{45-n}]$ for $n = 16, 17, \ldots, 29$.

As a summary, the molecular eigenfunctions of the model boron rotor $^{11}B^+_{13}$ are

$$\begin{aligned} &\Phi^{\text{mol}}_{nl,n'l'}(\xi;\Sigma_1,\Sigma_2,\Sigma_3,\Sigma_a,\Sigma_b,\ldots,\Sigma_j) \\ &\quad = \Phi_{nl}(\xi)\,\Phi^{\text{nu.sp}}_{n'l'}(\Sigma_1,\Sigma_2,\Sigma_3,\Sigma_a,\Sigma_b,\ldots,\Sigma_j) \end{aligned} \tag{41}$$

with $n = 0, 1, 2, \ldots, 29$, $(n+n')\bmod 30 = 15$, and $l = 0, 1, \ldots, l' = 1, 2, \ldots, N^{\text{nu.sp}}(\Gamma_{n'})$.

D. Mean values of the contorsional momenta of the nuclear spin isomers of $^{11}B^+_{13}$

The quantum mechanical operator of the z-component of the contorsional angular momentum (i.e., the component perpendicular to the molecular x-y-plane of the oriented model rotor $^{11}B^+_{13}$) is conjugate to the contorsional coordinate ξ,

$$L_z = -i\,\hbar\frac{\partial}{\partial\xi}. \tag{42}$$

The contorsional symmetry of L_z is Γ_0. Hence the mean values of L_z for the contorsional eigenfunctions $\Phi_{nl}(\xi)$ of the nuclear spin isomers of $^{11}B^+_{13}$ labeled $\Gamma_n[\Gamma_{15-n}]$ ($n = 0, 1, 2, \ldots, 15$) or $\Gamma_n[\Gamma_{45-n}]$ ($n = 16, 17, \ldots, 29$) are evaluated as

$$\langle\Phi_{nl}|L_z|\Phi_{nl}\rangle = \sum_{k,k'} c_{k,nl} * c_{k',nl}\langle\phi_k|L_z|\phi'_k\rangle = \hbar\sum_k |c_{k,nl}|^2\,k. \tag{43}$$

The relation (13) implies that the mean values of the angular momenta of the degenerate levels E_{nl} and $E_{(30-n)l}$ of the nuclear spin isomers labeled $\Gamma_n[\Gamma_{15-n}]$ and $\Gamma_{30-n}[\Gamma_{15+n}]$, $n = 1, 2, \ldots, 14$, have opposite signs,

$$\begin{aligned} \langle\Phi_{nl}|L_z|\Phi_{nl}\rangle &= \hbar\sum_k |c_{k,nl}|^2 k \\ &= \hbar\sum_k |c_{-k,(30-n)l}|^2 k \quad (k \bmod 30 = n) \\ &= \hbar\sum_k |c_{k,(30-n)l}|^2(-k) \quad (k \bmod 30 = 30-n) \\ &= -\langle\Phi_{(30-n)l}|L_z|\Phi_{(30-n)l}\rangle \text{ for } n = 1, 2, \ldots, 14. \end{aligned} \tag{44}$$

For the non-degenerate levels E_{0l} and E_{15l} of the nuclear spin isomers $\Gamma_0[\Gamma_{15}]$ and $\Gamma_{15}[\Gamma_0]$ of $^{11}B^+_{13}$), the symmetry relations (14) and (15) of the coefficients imply that the mean contorsional angular momenta are equal to zero,

$$\langle\Phi_{0l}|L_z|\Phi_{0l}\rangle = \langle\Phi_{15l}|L_z|\Phi_{15l}\rangle = 0. \tag{45}$$

In particular, the mean contorsional angular momentum of the ground state of $^{11}B^+_{13}$ is equal to zero,

$$\langle\Phi_{00}|L_z|\Phi_{00}\rangle = 0. \tag{46}$$

The corresponding nuclear spin isomer has IRREPs $\Gamma_0[\Gamma_{15}]$.

III. RESULTS AND DISCUSSION

In Sec. III A, we shall first present the representative results for the contorsional eigenfunctions, the levels, the mean values of the contorsional angular momenta, and the contorsional [nuclear spin] IRREPs of the oriented model rotor $^{11}B^+_{13}$. In the second part, we shall discuss the consequences, i.e., the constraints of the nuclear spins imposed on laser induced contorsional transitions of $^{11}B^+_{13}$.

A. Contorsional eigenfunctions, levels, mean values of angular momenta, and IRREPs of the model rotor $^{11}B^+_{13}$

Selected solutions of the contorsional Schrödinger equation (10) are illustrated in Fig. 3. Specifically, Fig. 3 shows the four non-degenerate real-valued contorsional eigenfunctions $\Phi_{nl}(\xi)$ and eigenenergies E_{nl} of the oriented model rotor $^{11}B^+_{13}$, at the bottoms (n, $l = 0$, 0 and 15, 1) and at the tops (n, $l = 15$, 0 and 0, 1) of the lowest ($l = 0$) and first excited ($l = 1$) energy bands. The corresponding numbers of nodes of the wavefunctions (excluding the nodes at the edges of the cyclic domain $0 \leqslant \xi \leqslant 2\pi$) increase from 0 (for n, $l = 0$, 0) via 29, 30 (for n, $l = 15$, 0 and 1, 0) to 59 (for n, $l = 0$, 1). The contorsional [and nuclear spin] IRREPs are $\Gamma_0[\Gamma_{15}]$, $\Gamma_{15}[\Gamma_0]$, $\Gamma_{15}[\Gamma_0]$, and $\Gamma_0[\Gamma_{15}]$, respectively. These examples show that the combination of IRREPs $\Gamma_0[\Gamma_{15}]$ may be assigned either to the lowest or to the highest levels of the energy bands and vice versa for the "opposite" combination $\Gamma_{15}[\Gamma_0]$.

The complete set of all energies E_{nl} of the lowest ($l = 0$) and first excited ($l = 1$) energy bands of the oriented model rotor $^{11}B^+_{13}$ is shown in Fig. 4 (these results agree with those of Ref. 20), together with the new results for the mean values of the contorsional angular momenta $\langle\Phi_{nl}|L_z|\Phi_{nl}\rangle$ and assignments of the IRREPs $\Gamma_n[\Gamma_{n'}]$. The numerical results confirm

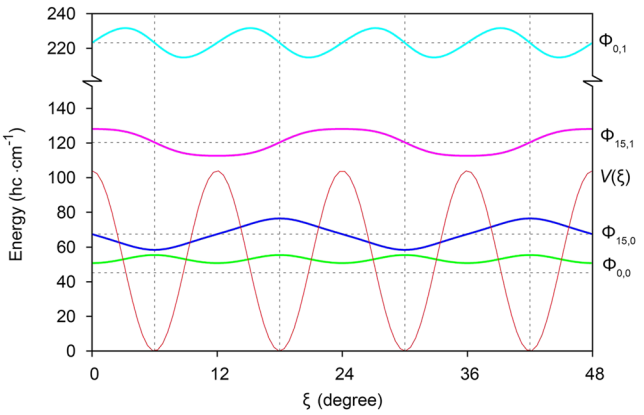

FIG. 3. Non-degenerate, real-valued contorsional eigenfunctions $\Phi_{nl}(\xi)$ of the oriented model rotor $^{11}B^{+}_{13}$, at the bottoms (n, l = 0, 0 and 15, 1) and at the tops (n, l = 15, 0 and 0, 1) of the lowest (l = 0) and first excited (l = 1) energy bands. Horizontal base lines of the wavefunctions are drawn at the related contorsional eigenenergies E_{nl} below and above the barriers of the cyclic contorsional model potential $V(\xi)$, respectively. For clarity, the results are shown just for the rather small contorsional domain $0° \leqslant \xi \leqslant 48°$, with four potential minima supporting the global minimum structures GM_1–GM_4.

the non-degeneracy of the levels at the bottom and top of the energy bands (n = 0, 15) and the degeneracy $E_{nl} = E_{(30-n),l}$ [Eq. (12)] of the other levels. Likewise, they confirm that the mean values of the contorsional angular momenta of the non-degenerate levels at the top and bottom of the energy bands are equal to zero, cf. Eq. (45), whereas the complementary pairs of degenerate levels have opposite non-zero values $\langle\Phi_{nl}|L_z|\Phi_{nl}\rangle = -\langle\Phi_{(30-n)l}|L_z|\Phi_{(30-n)l}\rangle$ [cf. Eq. (44)].

B. Constraints on laser induced transitions in the model rotor $^{11}B^{+}_{13}$ imposed by nuclear spin conservation

The results shown in Fig. 4 imply huge consequences for laser-induced contorsional transitions. As discussed in detail in Ref. 22, we assume that the corresponding laser pulses have much shorter durations than any intra-molecular nuclear spin-flips. As the first consequence, the IRREP $\Gamma_{n'}$ of the nuclear

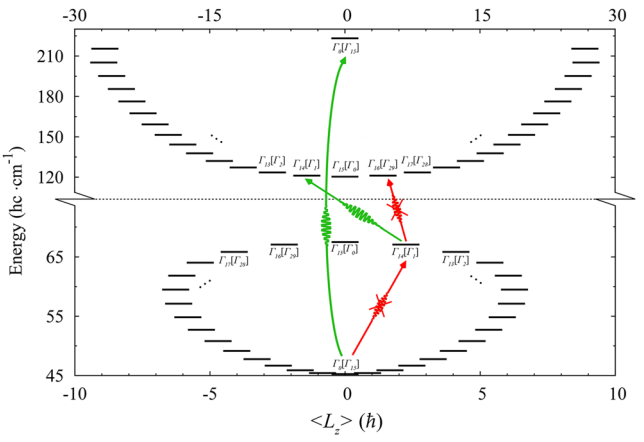

FIG. 4. Energies E_{nl}, irreducible representations (IRREPs) $\Gamma_n[\Gamma_{n'}]$ for the contorsion [and nuclear spin], and mean values of the contorsional angular momenta $\langle L_z\rangle = \langle\Phi_{nl}|L_z|\Phi_{nl}\rangle$ of the eigenstates $|\Phi_{nl}\rangle$ of the oriented model rotor $^{11}B^{+}_{13}$. The arrows illustrate that laser induced transitions must conserve the IRREPs—all other transitions are blocked by nuclear spins.

spins of the initial state is conserved during the laser-induced transition. As explained in Sec. II C, the second consequence is that the contorsional IRREP Γ_n is also conserved, subject to the constraint $(n + n') \bmod 30 = 15$. The third consequence is that laser pulses conserve the IRREP labels $\Gamma_n[\Gamma_{n'}]$ of the nuclear spin isomers.

Let us now consider some special consequences of these general rules. First we consider the boron rotor in its ground state $\Gamma_0[\Gamma_{15}]$. This state is non-degenerate and its mean value of the contorsional angular momentum is equal to zero [cf. Eq. (46)]. Figure 4 illustrates that irrespective of the specific design of the laser pulse, one cannot induce any contorsional intra-band transitions because all the thirty eigenstates of the energetic ground state band have different IRREPs.[22] As an example, Fig. 4 shows one of the hypothetical transitions—i.e., the transition from the ground state labeled $\Gamma_0[\Gamma_{15}]$ to the excited state labeled $\Gamma_{14}[\Gamma_1]$—which is blocked by conservation of nuclear spins. Likewise, the first excited energy band carries again thirty states, all with different IRREPs.[22] This means that one can induce one and only one inter-band transition (out of 30 choices) between the ground and first excited bands, starting from the ground state, namely, the transition that conserves the IRREP $\Gamma_0[\Gamma_{15}]$. The only possible transition from the ground state to any of the 59 excited states of the ground and first excited energy bands is, therefore, to the non-degenerate state at the top of the first excited state—this transition is indicated by an arrow in Fig. 4. Now since the target state is non-degenerate, its mean value of contorsional angular momentum is again equal to zero. By analogous extrapolation, the only possible laser-induced transitions from the ground state to any target states of the second, third, etc. excited bands will again end up in non-degenerate states labeled by the IRREP $\Gamma_0[\Gamma_{15}]$, with the mean value of the contorsional angular momentum equal to zero. This means that it is impossible to ignite any rotation of the molecular wheel of the model rotor $^{11}B^{+}_{13}$ with respect to its pseudo-rotating bearing by means of laser induced intra- or inter-band transitions: this hypothetical process, laser-induced ignition of contorsion in the model rotor $^{11}B^{+}_{13}$, is blocked by conservation of nuclear spins.

This nuclear spin blockade holds regardless of whether the transitions are dipole-allowed or dipole-forbidden. In fact, dipole selection rules could only further restrict any hypothetical transition from the non-contorting ground state to excited contorsional states. Yet, these restrictions might be overcome, for example, by using ultrashort intense laser pulses.[24,25] Thus, it is the nuclear spin that ultimately blocks transitions from the non-contorting ground state to contorting excited states.

An immediate consequence of nuclear spin blockade of laser-induced contorsional ignition of the model rotor $^{11}B^{+}_{13}$ is that the reverse process is also impossible. For example, let us assume that the rotor is in one of its degenerate excited states that carry a non-zero mean value of contorsional angular momentum, e.g., in the state labeled by IRREPs $\Gamma_{14}[\Gamma_1]$ [cf. Fig. 4]. Then conservation of nuclear spins blocks laser-induced retardation of the contorsion to zero mean value of contorsional angular momentum of $^{11}B^{+}_{13}$ in its ground state labeled $\Gamma_0[\Gamma_{15}]$.

Figure 4 illustrates examples of complementary rather general constraints on laser induced transitions in the model rotor $^{11}B_{13}^{+}$ imposed by conservation of nuclear spins. First, let us assume that the model rotor is prepared in a degenerate excited state with a non-zero mean value of contorsional angular momentum, say, again in the state labeled $\Gamma_{14}[\Gamma_1]$ [cf. Fig. 4]. Any inter-band transition to the next higher energy band must conserve the IRREP $\Gamma_{14}[\Gamma_1]$. Figure 4 shows that there is one and only one target state (out of thirty choices) that satisfies this condition—all other inter-band transitions are prohibited by conservation of nuclear spin. Figure 4 also discovers a fascinating effect: this transition changes the direction of the contorsion, from clockwise to anti-clockwise, or vice versa. The reason is that the mean values of the contorsional momenta $\langle\Phi_{n0}|L_z|\Phi_{n0}\rangle$ and $\langle\Phi_{n1}|L_z|\Phi_{n1}\rangle$ of eigenstates Φ_{n0} and Φ_{n1} in the ground and first excited energy bands with the same IRREPs $\Gamma_n[\Gamma_{n'}]$ are opposite (cf. Fig. 4). As an outlook, the change in the direction of the contorsion by inter-band transitions also suggests to design a laser pulse that transfers partial population from the initial state (such as the one labeled $\Gamma_{14}[\Gamma_1]$) of the ground energy band to the target state with the same IRREP in the first excited band. At the end of the laser pulse, the rotor is then prepared in a superposition of two states with contorsions in opposite directions such that the mean value of the contorsional momentum is equal to zero. Note that this type of superposition state is not a state at contorsional rest—it is just its mean value that is equal to zero.

Finally, Fig. 4 also suggests some consequences for the infrared (IR) spectroscopy of the boron rotor $^{11}B_{13}^{+}$ as follows: The traditional consideration of global minimum structures [with C_{2v} symmetry, cf. Fig. 2(b)] would predict that all thirty GM structures yield equivalent spectra—i.e., the spectral lines are thirtyfold degenerate. In particular, one should observe an IR absorption peak for the excitation of the normal mode with the lowest vibrational frequency, $\nu_1 \approx 135.2\ \mathrm{cm}^{-1}$—this is the mode that correlates with contorsion along ξ.[19,20] By contrast, the present consideration of cyclic contorsion along ξ, from one GM to all others, yields the splitting of the levels of the individual GMs. Such splittings are familiar, e.g., as tunneling doublets of molecules that possess two interacting GMs; compare the example of the tunneling inversion of ammonia. In the present case, thirty interacting GMs cause the corresponding sixteen-plet structures of the energy bands that are illustrated in Fig. 4, with fourteen doubly degenerate levels between two non-degenerate levels, representing $14 \times 2 + 2 = 30$ states in each energy band. Excitation of the ν_1 mode of the individual GM is thus replaced by inter-band excitation from the ground band to the first excited energy band for the contorsion along ξ that correlates with ν_1 vibration. Now conservation of nuclear spins blocks all hypothetical inter-band transitions, except the thirty transitions that conserve the IRREPs $\Gamma_n[\Gamma_{n'}]$ see also the supplementary material. Thus, the present investigation suggests that high resolution spectroscopy of $^{11}B_{13}^{+}$ should discover a set of sixteen transitions that correlate with ν_1 for the individual GM. Figure 4 reveals that due to conservation of the IRREPs, the lowest and highest frequencies of the sixteen-plet are $\nu_1(\Gamma_{15}[\Gamma_0]) = (120.4 - 67.5 = 52.9)\ \mathrm{cm}^{-1}$ and $\nu_1(\Gamma_0[\Gamma_{15}]) = (223.2 - 45.2 = 178.0)\ \mathrm{cm}^{-1}$ for the transitions that conserve the IRREPs $\Gamma_{15}[\Gamma_0]$ and $\Gamma_0[\Gamma_{15}]$ of the non-degenerate levels (cf. Ref. 20). Low resolution IR spectra would observe the corresponding apparent "broadening" of the "ν_1-transition." The total width of the apparent IR absorption line should be of the order of $(178.0 - 52.9 = 125.1)\ \mathrm{cm}^{-1}$, whereas the full width at half maximum should be of the order of $(125.1/2 \approx 60)\ \mathrm{cm}^{-1}$. The IR spectral window of the experimental method of Fagiani *et al.*[14] did not include the transitions with lowest frequencies; in particular, they were unable to observe or even resolve the "ν_1-transition(s)," but anyway, in the context of the present investigation, we consider it rewarding that the absorption peaks at higher frequencies are significantly broader than the spectral line widths; see also the discussion in Ref. 19.

IV. CONCLUSIONS

The present investigation shows that the challenge—or should we say the dream—to design laser pulses that could ignite contorsion of the model boron rotor $^{11}B_{13}^{+}$ is prohibited by conservation of nuclear spins. The reason for this nuclear spin blockade is as follows: We assume that initially, $^{11}B_{13}^{+}$ is prepared in its non-rotating ground state. This state is characterized by the specific combination of the IRREPs $\Gamma_0[\Gamma_{15}]$ for contorsion [and nuclear spin]. All excited states with non-zero contorsional angular momentum have different IRREPs $\Gamma_{n\neq0}[\Gamma_{n'\neq15}]$, or, turning the table, all excited states with IRREPs $\Gamma_0[\Gamma_{15}]$ have zero mean values of contorsional angular momentum. But laser-induced transitions from the ground state ($\Gamma_0[\Gamma_{15}]$) to excited states $\Gamma_n[\Gamma_{n'}]$ must conserve the IRREPs because otherwise any hypothetical transition $\Gamma_0[\Gamma_{15}] \rightarrow \Gamma_{n\neq0}[\Gamma_{n'\neq15}]$ would require nuclear spin flips that cannot be realized during the laser pulse. As a consequence, the conservation of nuclear spins restricts laser-induced transitions from the ground state with IRREPs $\Gamma_0[\Gamma_{15}]$ to excited target states with the same IRREPs, which means with the same, namely, zero, contorsional angular momentum. In brief, conservation of nuclear spins blocks laser ignition of contorsion in the model rotor $^{11}B_{13}^{+}$.

This paper also discovers various other constraints on laser-induced transitions that are imposed by conservation of nuclear spin. For example, laser pulses can change clockwise to counter-clockwise contorsions, or vice versa, but they cannot stop them.

The results have been derived in the frame of the model for contorsions of $^{11}B_{13}^{+}$ which has been developed in Refs. 19 and 20 supplemented by an important extension which accounts for effects of nuclear spins.[22] In particular, the spin statistics theorem allows only thirty (out of $30^2 = 900$) special combinations of the IRREPs of the contorsional times the nuclear spin functions. Analogous to the fact that one cannot design any laser pulse that would induce a transition from the non-rotating ground state of hydrogen ($JM = 00$, $I_{\mathrm{tot}} = 0$; *para*-H_2) to any rotating state of *ortho*-H_2 (see Fig. 1), conservation of nuclear spin makes it impossible to design any laser pulse that would excite the non-contorting ground state of $^{11}B_{13}^{+}$ (IRREP $\Gamma_0[\Gamma_{15}]$) to any contorting state (IRREP $\Gamma_{n\neq0}[\Gamma_{n'\neq15}]$) (see Fig. 4). The rule for hydrogen holds irrespective of the complementary vibrational degree of freedom. As a working

hypothesis, the present rule for $^{11}B_{13}^+$ should also hold irrespective of the complementary vibrational degrees of freedom. In any case, the present results suggest that proper modeling of the boron rotors must take nuclear spin symmetry into account—otherwise one may miss important effects such as nuclear spin blockade of ignition of contorsions. In general, our findings confirm that molecular symmetries are important in quantum reaction dynamics.[44]

SUPPLEMENTAL MATERIAL

See supplementary material for the statistical weights of the nuclear spin isomers of $^{11}B_{13}^+$ and the model for contorsional eigenstates of $^{11}B_{13}^+$ in magnetic field.

ACKNOWLEDGMENTS

We thank Professor Si-Dian Li (Taiyuan) for his encouraging enthusiasm and Professor Martin Quack (Zürich) for advice on the proper units.[45] Thomas Grohmann acknowledges support by the Deutsche Forschungsgemeinschaft (Project No. GR 4508/2-1). This work also profits from financial support in part by the National Key Research and Development Program of China (No. 2017YFA0304203), the program for Changjiang Scholars and Innovative Research Team (No. IRT_17R70), the 111 project (Grant No. D18001), the Fund for Shanxi "1331 Project" Key Subjects, and the National Natural Science Foundation of China (No. 11434007).

APPENDIX: THE GENERATOR OF THE CYCLIC MOLECULAR SYMMETRY GROUP $C_{30}(M)$ OF $^{11}B_{13}^+$

The generator g of the cyclic MS group $C_{30}(M)$ may be determined with help of Fig. 5 as follows: Fig. 5(a) shows the delocalized structure of $^{11}B_{13}^+$ which is due to the superposition of altogether thirty global minimum structures GM, in the laboratory frame. Two of them, namely, GM_1 and GM_2 are marked by red dots and by open circles in Fig. 5(a). Figures 5(b) and 5(c) show GM_1 and GM_2 with labels 1, 2, 3 and a, b, c, . . ., j attached to the nuclei of the inner wheel and of the outer bearing, in clockwise orders. The generator g transfers GM_1 into GM_2,

$$g\mathrm{GM}_1 = \mathrm{GM}_2. \tag{A1}$$

This is achieved by concerted shifts of all nuclei along the contorsional coordinate ξ,

$$g\xi = \xi + \Delta\xi, \Delta\xi = 2\pi/30. \tag{A2}$$

Specifically, when ξ increases by the small contorsional shift $\Delta\xi$, the individual nuclei of the wheel move versus the bearing by small steps along paths that are approximately circular, whereas the nuclei of the bearing move along pseudorotational paths. The rather small steps along these paths are obvious from Fig. 5(a). Now, even though the shifts of the individual nuclei are small, the net effect is a rearrangement of the overall shape of the rotor $^{11}B_{13}^+$ that appears *as if* it has been rotated by a rather large angle. In order to recognize this *apparent* rotation of $^{11}B_{13}^+$, we have added dashed arrows in Figs. 5(b) and 5(c) that represent the symmetry axes of GM_1

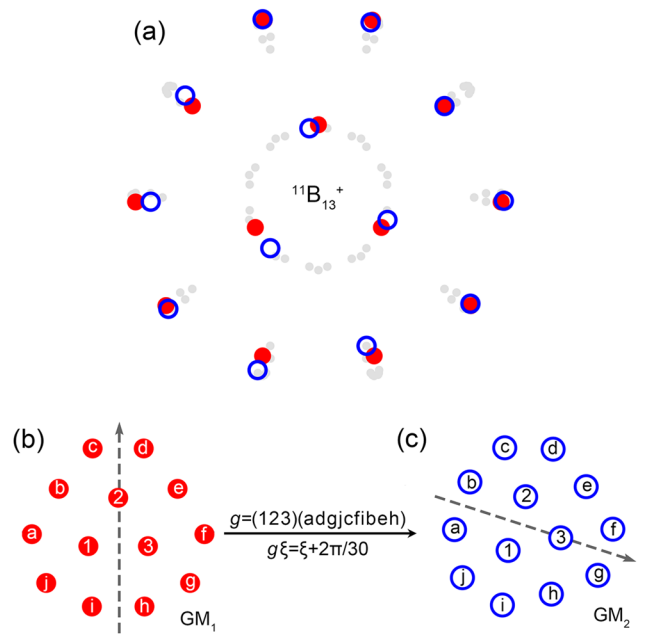

FIG. 5. (a) Delocalized structure of $^{11}B_{13}^+$ as superposition of thirty global minimum structures GM_l, $l = 0, 1,2,3, \ldots, 29$. As an example, GM_1 and GM_2 are illustrated by red dots and by open circles in panels (b) and (c). (b) Global minimum structure GM_1 of $^{11}B_{13}^+$ with the nuclei of the inner wheel and the outer bearing labeled 1, 2, 3 and a, b, c, . . ., j, respectively. As a guide to the eye, the dashed arrow indicates the symmetry axis of the molecular point group C_{2v} of GM_1 of $^{11}B_{13}^+$. (c) The same as (b), but for GM_2.

and GM_2. The symmetry axis of GM_1 is replaced by the symmetry axis of GM_2 *as if* it has been rotated by a rather large angle.

Now let us consider the effect of g in the frames of the global minimum structures GM_m. For convenience, we attach right-handed Cartesian coordinates x_m, y_m, z_m to GM_m such that x_m and y_m are in the molecular plane and x_m points along the C_{2v} symmetry axis and z_m is perpendicular to the molecular plane. The values x_{mk}, y_{mk}, z_{mk} (=0) of the nuclear coordinates at the nuclei $k = 1, 2, 3, a, b, \ldots, j$ are the same for all GM_m. Let us focus on the nucleus that sits of the symmetry axis. In GM_1, this is the nucleus labeled 2, whereas in GM_2, it is nucleus 3. This means that in the molecular frame, the effect of g is to replace nucleus 2 by 3. Likewise, in clockwise order, the nuclei 3 and 1 of GM_1 are replaced by nuclei 1 and 2 in GM_2 [cf. Figs. 5(b) and 5(c)]. Altogether, the replacement of the nuclei 2, 3, and 1 in GM_1 by 3, 1, and 2 in GM_2 is represented by the permutation

$$\mathrm{P_{in}} = (123) \tag{A3}$$

of the nuclei of the inner wheel.

Next, let us investigate the effect of g on the nuclei of the bearing, again in the molecular frame. Let us focus on the two nuclei of the bearing that sit to the left and to the right of the arrow head of the symmetry axis. In GM_1, these are the nuclei labeled c and d, whereas in GM_2, these are the nuclei labeled f and g. Likewise, in clockwise order, the nuclei labeled e, f, g, h, i, j, a, and b in GM_1 are replaced by nuclei h, i, j, a, b, c, d, and e in GM_2. Altogether, the replacement of the nuclei c, d, e, f, g, h, i, j, a, and b in GM_1 by f, g, h, i, j, a, b, c, d, and e in GM_2 is described by the permutation

$$\mathrm{P_{out}} = (\mathrm{adgjcfibeh}) \tag{A4}$$

of the nuclei of the bearing. Consequently, we have

$$g = P_{out}\, P_{in} = (123)(adgjcfibeh) \tag{A5}$$

q. e. d.

[1] G. S. Kottas, L. I. Clarke, D. Horinek, and J. Michl, Chem. Rev. **105**, 1281 (2005).
[2] S. P. Fletcher, F. Dumur, M. M. Pollard, and B. L. Feringa, Science **310**, 80 (2005).
[3] J. Wang and B. L. Feringa, Science **331**, 1429 (2011).
[4] B. L. Feringa, Angew. Chem., Int. Ed. **56**, 11060 (2017).
[5] Y. Fujimura, L. González, D. Kröner, J. Manz, I. Mehdaoui, and B. Schmidt, Chem. Phys. Lett. **386**, 248 (2004).
[6] M. Yamaki, S. Nakayama, K. Hoki, H. Kono, and Y. Fujimura, Phys. Chem. Chem. Phys. **11**, 1662 (2009).
[7] G. Pérez-Hernández, A. Pelzer, L. González, and T. Seideman, New J. Phys. **12**, 075007 (2010).
[8] H. Isobe, K. Nakamura, S. Hitosugi, S. Sato, H. Tokoyama, H. Yamakado, K. Ohno, and H. Kono, Chem. Sci. **6**, 2746 (2015).
[9] Y.-J. Wang, X.-Y. Zhao, Q. Chen, H.-J. Zhai, and S.-D. Li, Nanoscale **7**, 16054 (2015).
[10] S. Jalife, L. Liu, S. Pan, J. L. Cabellos, E. Osorio, C. Lu, T. Heine, K. J. Donald, and G. Merino, Nanoscale **8**, 17639 (2016).
[11] G. Martínez-Guajardo, A. P. Sergeeva, A. I. Boldyrev, T. Heine, J. M. Ugalde, and G. Merino, Chem. Commun. **47**, 6242 (2011).
[12] J. Zhang, A. P. Sergeeva, M. Sparta, and A. N. Alexandrova, Angew. Chem., Int. Ed. **51**, 8512 (2012).
[13] G. Merino and T. Heine, Angew. Chem., Int. Ed. **51**, 10226 (2012).
[14] M. R. Fagiani, X. Song, P. Petkov, S. Debnath, S. Gewinner, W. Schöllkopf, T. Heine, A. Fielicke, and K. R. Asmis, Angew. Chem., Int. Ed. **56**, 501 (2017).
[15] Y.-J. Wang, X.-R. You, Q. Chen, L.-Y. Feng, K. Wang, T. Ou, X.-Y. Zhao, H.-J. Zhai, and S.-D. Li, Phys. Chem. Chem. Phys. **18**, 15774 (2016).
[16] W. Huang, A. P. Sergeeva, H.-J. Zhai, B. B. Averkiev, L.-S. Wang, and A. I. Boldyrev, Nat. Chem. **2**, 202 (2010).
[17] J. O. C. Jiménez-Halla, R. Islas, T. Heine, and G. Merino, Angew. Chem., Int. Ed. **49**, 5668 (2010).
[18] L. Liu, D. Moreno, E. Osorio, A. C. Castro, S. Pan, P. K. Chattaraj, T. Heine, and G. Merino, RSC Adv. **6**, 27177 (2016).
[19] Y. Yang, D. Jia, Y.-J. Wang, H.-J. Zhai, Y. Man, and S.-D. Li, Nanoscale **9**, 1443 (2017).
[20] D. Jia, J. Manz, and Y. Yang, AIP Adv. **8**, 045222 (2018).
[21] J. Manz, J. Am. Chem. Soc. **102**, 1801 (1980).
[22] T. Grohmann and J. Manz, Mol. Phys. **116**, 2538 (2018).
[23] P. R. Bunker and P. Jensen, *Molecular Symmetry and Spectroscopy* (NRC Research Press, 2006).
[24] G. K. Paramonov, Chem. Phys. Lett. **411**, 350 (2005).
[25] C. J. Eyles and M. Leibscher, J. Chem. Phys. **139**, 104315 (2013).
[26] A. P. Sergeeva, I. A. Popov, Z. A. Piazza, W.-L. Li, C. Romanescu, L.-S. Wang, and A. I. Boldyrev, Acc. Chem. Res. **47**, 1349 (2014).
[27] L.-S. Wang, Int. Rev. Phys. Chem. **35**, 69 (2016).
[28] M. Tinkham, *Group Theory and Quantum Mechanics* (McGraw-Hill, 1964).
[29] W. M. Haynes, *CRC Handbook of Chemistry and Physics* (CRC Press, 2014).
[30] J. O. Hirschfelder and J. S. Dahler, Proc. Natl. Acad. Sci. U. S. A. **42**, 363 (1956).
[31] D. W. Jepsen and J. O. Hirschfelder, Proc. Natl. Acad. Sci. U. S. A. **45**, 249 (1959).
[32] J. O. Hirschfelder, Int. J. Quantum Chem. **3**, 17 (1969).
[33] T. Bredtmann, D. J. Diestler, S.-D. Li, J. Manz, J. F. Pérez-Torres, W.-J. Tian, Y.-B. Wu, Y. Yang, and H.-J. Zhai, Phys. Chem. Chem. Phy. **17**, 29421 (2015).
[34] C. Adamo and V. Barone, J. Chem. Phys. **110**, 6158 (1999).
[35] F. Weigend and R. Ahlrichs, Phys. Chem. Chem. Phys. **7**, 3297 (2005).
[36] M. J. Frisch, G. W. Trucks, H. B. Schlegel, G. E. Scuseria, M. A. Robb, J. R. Cheeseman, G. Scalmani, V. Barone, B. Mennucci, G. A. Petersson, H. Nakatsuji, M. Caricato, X. Li, H. P. Hratchian, A. F. Izmaylov, J. Bloino, G. Zheng, J. L. Sonnenberg, M. Hada, M. Ehara, K. Toyota, R. Fukuda, J. Hasegawa, M. Ishida, T. Nakajima, Y. Honda, O. Kitao, H. Nakai, T. Vreven, J. A. Montgomery, Jr., J. E. Peralta, F. Ogliaro, M. Bearpark, J. J. Heyd, E. Brothers, K. N. Kudin, V. N. Staroverov, R. Kobayashi, J. Normand, K. Raghavachari, A. Rendell, J. C. Burant, S. S. Iyengar, J. Tomasi, M. Cossi, N. Rega, J. M. Millam, M. Klene, J. E. Knox, J. B. Cross, V. Bakken, C. Adamo, J. Jaramillo, R. Gomperts, R. E. Stratmann, O. Yazyev, A. J. Austin, R. Cammi, C. Pomelli, J. W. Ochterski, R. L. Martin, K. Morokuma, V. G. Zakrzewski, G. A. Voth, P. Salvador, J. J. Dannenberg, S. Dapprich, A. D. Daniels, Ö. Farkas, J. B. Foresman, J. V. Ortiz, J. Cioslowski, and D. J. Fox, GAUSSIAN 09 Revision E.01, Gaussian, Inc., Wallingford CT, 2009.
[37] R. McWeeny, *Symmetry: An Introduction to Group Theory and Its Applications* (Courier Corporation, 2002).
[38] M. H. Levitt, *Spin Dynamics: Basics of Nuclear Magnetic Resonance* (Wiley-VCH, 2008).
[39] P. R. Bunker and P. Jensen, *Fundamentals of Molecular Symmetry* (Institute of Physics Publishing, 2008).
[40] Z.-D. Sun, K. Takagi, and F. Matsushima, Science **310**, 1938 (2005).
[41] J. T. Hougen and T. Oka, Science **310**, 1913 (2005).
[42] P. L. Chapovsky, V. V. Zhivonitko, and I. V. Koptyug, J. Phys. Chem. A **117**, 9673 (2013).
[43] Z.-D. Sun, M. Ge, and Y. Zheng, Nat. Commun. **6**, 6877 (2015).
[44] M. Quack, Mol. Phys. **34**, 477 (1977).
[45] E. R. Cohen, T. Cvitaš, J. G. Frey, B. Holmström, K. Kuchitsu, R. Marquardt, I. Mills, F. Pavese, M. Quack, J. Stohner, H. L. Strauss, M. Takami, and A. J. Thors, *Quantities, Units and Symbols in Physical Chemistry*, 3rd ed. (IUPAC, RSC Publishing, 2007).